ACS APPLIED MATERIALS & INTERFACES

Research Article

www.acsami.org

Rapid Exchange between Atmospheric CO_2 and Carbonate Anion Intercalated within Magnesium Rich Layered Double Hydroxide

Pathik Sahoo,[†] Shinsuke Ishihara,*[,‡] Kazuhiko Yamada,[§] Kenzo Deguchi,[∥] Shinobu Ohki,[∥] Masataka Tansho,[∥] Tadashi Shimizu,[∥] Nii Eisaku,[⊥] Ryo Sasai,[⊥] Jan Labuta,[†] Daisuke Ishikawa,[†] Jonathan P. Hill,[†] Katsuhiko Ariga,[†] Bishnu Prasad Bastakoti,[†] Yusuke Yamauchi,[†] and Nobuo Iyi*[,†]

[†]International Center for Materials Nanoarchitectonics (MANA), National Institute for Materials Science (NIMS), 1-1 Namiki, Tsukuba, Ibaraki 305-0044, Japan

[‡]Functional Geomaterials Group, National Institute for Materials Science (NIMS), 1-1 Namiki, Tsukuba, Ibaraki 305-0044, Japan

[§]Department of Chemistry and Materials Science, Graduate School of Science and Engineering, Tokyo Institute of Technology, Ookayama, Meguro, Tokyo 152-8552, Japan

[∥]High Field NMR Group, National Institute for Materials Science (NIMS), 3-13 Sakura, Tsukuba, Ibaraki 305-0003, Japan

[⊥]Department of Physics and Materials Science, Interdisciplinary Graduate School of Science and Engineering, Shimane University, 1060 Nishikawatsu, 690-8504 Matsue, Japan

ABSTRACT: The carbon cycle, by which carbon atoms circulate between atmosphere, oceans, lithosphere, and the biosphere of Earth, is a current hot research topic. The carbon cycle occurring in the lithosphere (e.g., sedimentary carbonates) is based on weathering and metamorphic events so that its processes are considered to occur on the geological time scale (i.e., over millions of years). In contrast, we have recently reported that carbonate anions intercalated within a hydrotalcite ($Mg_{0.75}Al_{0.25}(OH)_2(CO_3)_{0.125}{\cdot}yH_2O$), a class of a layered double hydroxide (LDH), are dynamically exchanging on time scale of hours with atmospheric CO_2 under ambient conditions. (Ishihara et al., *J. Am. Chem. Soc.* **2013**, *135*, 18040−18043). The use of ^{13}C-labeling enabled monitoring by infrared spectroscopy of the dynamic exchange between the initially intercalated ^{13}C-labeled carbonate anions and carbonate anions derived from atmospheric CO_2. In this article, we report the significant influence of Mg/Al ratio of LDH on the carbonate anion exchange dynamics. Of three LDHs of various Mg/Al ratios of 2, 3, or 4, magnesium-rich LDH (i.e., Mg/Al ratio = 4) underwent extremely rapid exchange of carbonate anions, and most of the initially intercalated carbonate anions were replaced with carbonate anions derived from atmospheric CO_2 within 30 min. Detailed investigations by using infrared spectroscopy, scanning electron microscopy, powder X-ray diffraction, elemental analysis, adsorption, thermogravimetric analysis, and solid-state NMR revealed that magnesium rich LDH has chemical and structural features that promote the exchange of carbonate anions. Our results indicate that the unique interactions between LDH and CO_2 can be optimized simply by varying the chemical composition of LDH, implying that LDH is a promising material for CO_2 storage and/or separation.

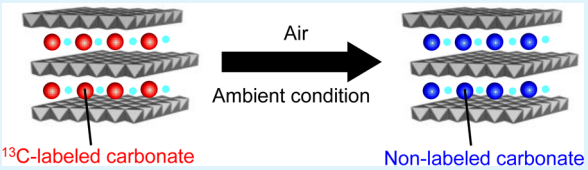

KEYWORDS: *clay mineral, layered double hydroxide, carbon dioxide, carbonate, anion exchange, isotope*

INTRODUCTION

Layered double hydroxide (LDH) is a clay mineral of general chemical formula of $M^{II}_{1-x}M^{III}_x(OH)_2(A^{n-})_{x/n}{\cdot}yH_2O$, where M^{II}, M^{III}, and A^{n-} are respectively a divalent metal cation, a trivalent metal cation, and a counteranion, and x is in the range of 0.2−0.33.[1,2] LDHs are composed of positively charged brucite-like metal hydroxide layers with water and charge-balancing anions located in the interlayer. Several types of LDHs are available naturally,[3] while LDH can also be synthesized in the laboratory.[4,5] It is thought that any combination of M^{II} and M^{III} is available in LDHs provided that the ionic radii of M^{II} and M^{III} are similar to that of Mg^{2+}.[6] Thus, LDHs have attracted interest because of their highly tunable chemical composition, which has enabled the design of functional LDHs suitable as anion exchange media,[7−10] adsorbents,[11−16] catalysts,[17−23] actuators,[24] hybrid materials,[25−28] separation systems,[29] drug delivery systems,[30,31] and so forth.

In our recent work, we have shown that carbonate anions contained in the interlayers of hydrotalcite ($Mg_{0.75}Al_{0.25}(OH)_2(CO_3)_{0.125}{\cdot}yH_2O$) undergo dynamic exchange with carbonate anions derived from atmospheric CO_2 even under ambient conditions, and that this process is complete in a few days.[32] In that case, ^{13}C-labeled carbonate anions ($^{13}CO_3^{2-}$) were used to allow differentiation by infrared (IR) spectroscopy between the initially intercalated ^{13}C-labeled carbonate anions and atmospheric-CO_2-derived (composed mostly of ^{12}C) carbonate anions (Figure 1). This finding

Received: September 4, 2014
Accepted: October 2, 2014
Published: October 2, 2014

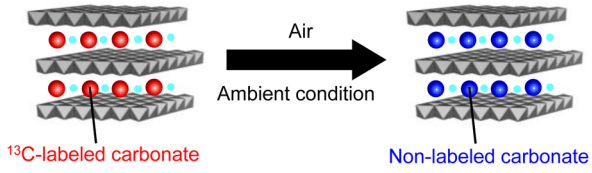

Figure 1. Dynamic exchange of carbonate anions of LDH with atmospheric CO_2.

conflicts with the then prevailing opinion that the carbon cycle[33] of carbonate solids (e.g., limestone) is based solely on weathering and metamorphic events, which occur over millions of years.[34,35] The dynamic exchange of carbonate anions observed uniquely for LDH is of great potential for various applications including for CO_2 separation and/or storage. Although anion exchange properties of LDHs suspension (i.e., at solid–liquid interface) have been investigated for decades,[7−10] anion exchange of LDHs at solid–gas interface is rarely investigated. The main purpose of this work is to probe the relationship existing between the chemical composition of LDHs and the exchange between atmospheric CO_2 and carbonate anions. Thus, we have prepared three types of LDHs with Mg/Al ratios of 2, 3, or 4 by coprecipitation method, and investigated the influence of Mg/Al ratio of LDH on carbonate anion exchange by using IR spectroscopy, scanning electron microscopy (SEM), powder X-ray diffraction (XRD), elementary analysis, adsorption, thermo gravimetric (TG) analysis, and solid-state NMR.

RESULTS AND DISCUSSION

Synthesis. The synthetic procedure for preparation of LDHs is shown in Scheme 1. First, carbonate-type LDHs with

Scheme 1. Synthesis of LDHs with Different Mg/Al Ratios and Interlayer Anions[a]

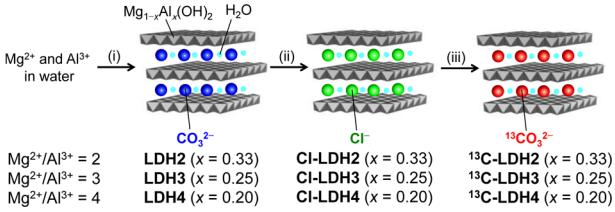

[a](i) Na_2CO_3 aq., 75 °C, pH = 12. (ii) HCl in propanol, 25 °C. (iii) ^{13}C—Na_2CO_3 aq., 25 °C.

Mg/Al ratio of 2 (**LDH2**), 3 (**LDH3**), and 4 (**LDH4**) were prepared by a coprecipitation method.[36] Typically, an aqueous solution of Na_2CO_3 was slowly added to a mechanically stirred hot aqueous solution containing Mg^{2+} and Al^{3+} mixture (where Mg/Al ratio was controlled to be 2, 3, or 4). During addition of Na_2CO_3, pH of the solution was maintained at 12 by addition of aqueous NaOH solution. The reaction was aged for 17 h then the white precipitate was filtered and washed with pure water. Samples were dried under reduced pressure yielding **LDH2**, **LDH3**, or **LDH4**.

Carbonate anions contained in **LDH2**, **LDH3**, and **LDH4** were exchanged with chloride anions by applying alcoholic HCl.[37] IR signals due to carbonate anions (1360−1378 cm^{-1}) in **LDH2**, **LDH3**, and **LDH4** could not be observed after anion exchange, indicating that interlayer carbonate anions had been replaced with chloride anions. Subsequently, the interlayer chloride anions were exchanged with ^{13}C-labeled carbonate anions by applying an aqueous solution of $Na_2{}^{13}CO_3$ (99%, ^{13}C) yielding ^{13}C-labeled carbonate type LDHs (**^{13}C-LDH2**, **^{13}C-LDH3**, and **^{13}C-LDH4**).

Characterization. Synthetic LDHs were fully characterized (by using IR spectroscopy, SEM, powder XRD, elemental analysis, and TGA) revealing them to be typical layered double hydroxides. The chemical compositions of **LDH2−4** are summarized in Table 1.

Table 1. Chemical Composition of LDH2-4 at Various Relative Humidity (RH)

sample	RH (%)	chemical composition
LDH2	0	$Mg_{0.68}Al_{0.32}(OH)_2(CO_3)_{0.16}\cdot(H_2O)_{0.67}$
LDH2	25	$Mg_{0.68}Al_{0.32}(OH)_2(CO_3)_{0.16}\cdot(H_2O)_{0.74}$
LDH2	95	$Mg_{0.68}Al_{0.32}(OH)_2(CO_3)_{0.16}\cdot(H_2O)_{0.93}$
LDH3	0	$Mg_{0.75}Al_{0.25}(OH)_2(CO_3)_{0.125}\cdot(H_2O)_{0.73}$
LDH3	25	$Mg_{0.75}Al_{0.25}(OH)_2(CO_3)_{0.125}\cdot(H_2O)_{0.78}$
LDH3	95	$Mg_{0.75}Al_{0.25}(OH)_2(CO_3)_{0.125}\cdot(H_2O)_{1.00}$
LDH4	0	$Mg_{0.80}Al_{0.20}(OH)_2(CO_3)_{0.098}\cdot(H_2O)_{0.67}$
LDH4	25	$Mg_{0.80}Al_{0.20}(OH)_2(CO_3)_{0.098}\cdot(H_2O)_{0.75}$
LDH4	95	$Mg_{0.80}Al_{0.20}(OH)_2(CO_3)_{0.098}\cdot(H_2O)_{0.98}$

Infrared spectroscopy was utilized to confirm the synthesis of LDHs by coprecipitation and following anion exchange reactions (i.e., $CO_3^{2-} \rightarrow Cl^- \rightarrow {}^{13}CO_3^{2-}$). As shown in Figure 2a, IR spectra of **LDH2−4** are typical of carbonate-type LDHs,

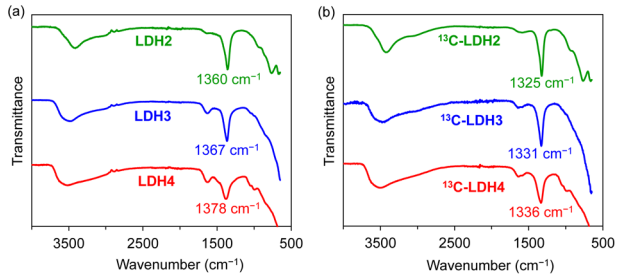

Figure 2. IR spectra of (a) **LDH2−4** and (b) **^{13}C-LDH2−4**.

which exhibit a C—O stretching vibration at around 1360−1378 cm^{-1}, bending vibration (scissoring) of water at around 1620 cm^{-1}, and a broad O—H stretching vibration at 3000−3700 cm^{-1}.[17,32,38] IR bands due to C—O stretching vibrations are shifted to lower wavenumber as the Mg/Al ratio decreases, suggesting that the carbonate anions in **LDH2−4** are in slightly different chemical environments. IR spectra of **^{13}C-LDH2**, **^{13}C-LDH3**, and **^{13}C-LDH4** are respectively identical to those of **LDH2**, **LDH3**, and **LDH4**, except that IR bands ascribed to C—O stretching are shifted to lower wavenumber (35−40 cm^{-1}) due to the ^{13}C isotope effect (Figure 2b).[32]

As shown in Figure 3a−c, SEM images of **LDH2−4** reveal their forms as plate-like structures, which are characteristic of layered double hydroxides. Diameters of the LDH plates are around 50−100 nm, which is smaller than those of well-crystallized LDHs usually obtained by the hydrothermal method (1−5 μm).[5] As seen in Figure 3d−f, the size and morphologies **^{13}C-LDH2−4** are similar to those of **LDH2−4**, so that anion exchange reactions did not cause significant damage to the LDH structures.

As shown in Figure 4a, XRD profiles of **LDH2−4** contain periodic diffraction patterns from d_{003} and d_{006}, which are

dx.doi.org/10.1021/am5060405 | ACS Appl. Mater. Interfaces 2014, 6, 18352−18359

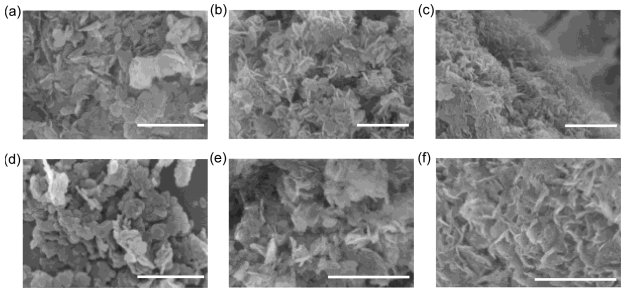

Figure 3. SEM images of (a) **LDH2**, (b) **LDH3**, (c) **LDH4**, (d) ^{13}**C-LDH2**, (e) ^{13}**C-LDH3**, and (f) ^{13}**C-LDH4**. Scale bars are all 500 nm.

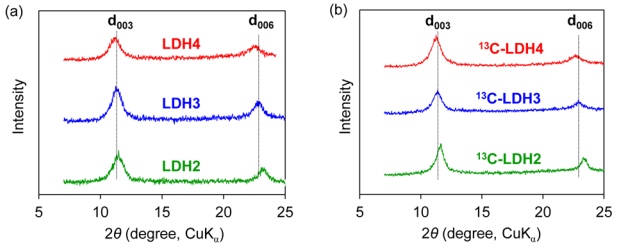

Figure 4. Powder XRD profiles of (a) **LDH2**–**4** and (b) ^{13}**C-LDH2**–**4** measured under dry N_2 atmosphere. The basal spacing was estimated as a double of d_{006}.

typical of layered structures. The basal spacings of these LDHs occur in the order **LDH2** (7.64 Å) < **LDH3** (7.77 Å) < **LDH4** (7.88 Å). As the quantity of Al^{3+} ions contained in the layered frameworks of LDH decrease (i.e., **LDH2** → **LDH4**), the positive charge density of the layered framework also decreases. Therefore, ionic interactions between the layered frameworks of **LDH4** and the interlayer carbonate anions is the weakest of the three LDHs described, resulting to the largest basal spacing. The basal spacing of ^{13}**C-LDH2**, ^{13}**C- LDH3**, and ^{13}**C-LDH4** were identical to those of **LDH2**, **LDH3**, and **LDH4**, respectively (Figure 4b).

Mg/Al ratios were determined to be 2.12 for **LDH2**, 2.99 for **LDH3**, and 4.08 for **LDH4** by using inductively coupled plasma atomic emission spectroscopy (ICP-AES) on homogeneous solutions of the LDH powders in 0.1 M aqueous HNO_3. Thus, the mixing ratios of Mg^{2+} and Al^{3+} used in the coprecipitation method (Scheme 1 (i)) are reflected in the final chemical compositions of **LDH2**–**4**.

TG analyses were conducted to determine the amount of interlayer water in **LDH2**–**4** (Figure 5). Just prior to analysis, LDHs were allowed to stand under a stream of dry N_2 at 40 °C for 6 h to remove weakly bound water. Then heating from 40 °C to ca. 250 °C, caused the removal of the interlayer water as well as physically adsorbed water. Further heating from ca. 250 °C to ca. 400 °C induces condensation of the layered framework as well as decarboxylation.[39−41] TG profiles of **LDH2**–**4** are in agreement with the previous report by Miyata et al. in that LDH of higher Mg/Al ratio tends to exhibit evaporation of interlayer water at lower temperature while dehydration and decarboxylation occur at higher temperature.[39] On the basis of the reduction in weight of LDHs upon heating from 40 to 250 °C (about 15% weight decrease), the quantities of interlayer water under dry conditions (i.e., relative humidity (RH) = 0%) were determined. In addition, the amount of water contained in LDHs at RH = 25 and 95% were measured based on increases in weight against that for under dry conditions. As summarized in Table 1, amounts of water contained in LDHs are independent of Mg/Al ratio, presumably because water molecules interact with hydroxide groups (OH). This result indicates that **LDH4** which contains the smallest amount of carbonate anions has the largest empty space in its interlayer region.

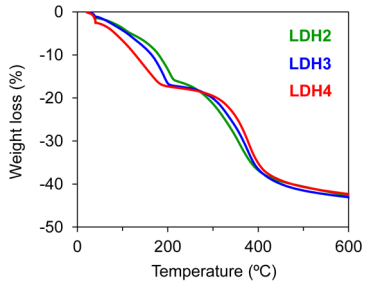

Figure 5. TG profiles of **LDH2**–**4** measured under dry N_2 flow. Heating rate was 10 °C/min.

Exchange of Carbonate Anions with Atmospheric CO_2. As shown in Figure 6a,b, the C—O vibration of ^{13}**C-LDH4** (indicated by asterisk) is shifted to higher wavenumber during a short period of time (ca. 30 min) if the sample is left in air (ca. 25 °C, RH = ca. 25%) indicating that ^{13}C-labeled carbonate anions in ^{13}**C-LDH4** rapidly exchanges with carbonate anions derived from atmospheric CO_2. Also, as is shown in Figure 6c, the rate of exchange of carbonate anions strongly depends on the Mg/Al ratio, and ^{13}**C-LDH2** demonstrates quite slow exchange. Considering the similarities in particle size (Figure 3d,e) and crystallinity (i.e., sharpness of XRD peaks in Figure 4b) of ^{13}**C-LDH2** and ^{13}**C-LDH3**, the slow exchange of ^{13}**C-LDH2** most likely originates from its chemical composition (i.e., Mg/Al ratio). Also, for all the LDHs studied here, exchange of carbonate anions became slower at

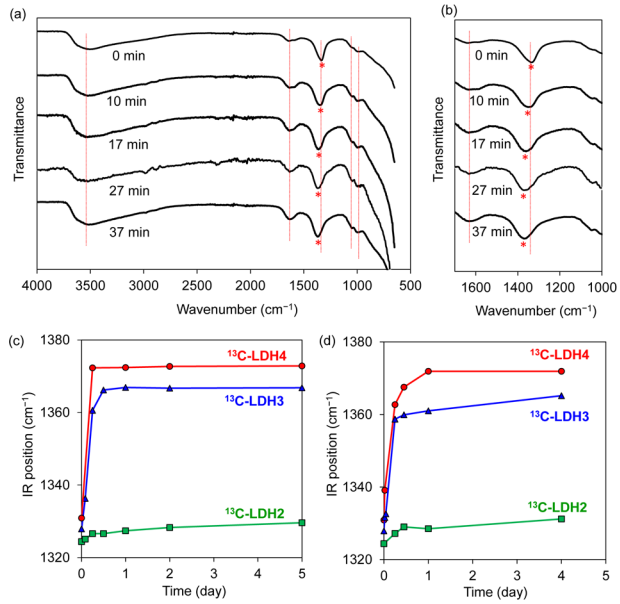

Figure 6. Variation of IR spectra of ^{13}**C-LDH4** in air (ca. 25 °C, RH = ca. 25%); (a) wide rage and (b) narrow range. (c) Variation of IR peak (C—O stretching) for ^{13}**C-LDH2**–**4** upon exposure to dry N_2 containing 395 ppm of CO_2 (RH = 1.8%). (d) Variation of IR peak (C—O stretching) for ^{13}**C-LDH2**–**4** upon exposure to wet N_2 containing 395 ppm of CO_2 (RH = 98%).

dx.doi.org/10.1021/am5060405 | ACS Appl. Mater. Interfaces 2014, 6, 18352−18359

high RH (Figure 6d). Nevertheless, exchange of carbonate anion in **^{13}C-LDH4** at RH = 98% was accomplished within 1 day.

Adsorption. According to N_2 adsorption−desorption isotherms measured at 77.35K and Brunauer−Emmett−Teller (BET) analyses, specific surface areas of LDHs were estimated to be 86 m^2/g for **LDH2**, 130 m^2/g for **LDH3**, and 81 m^2/g for **LDH4**(Figure 7a−c). These values of specific surface areas

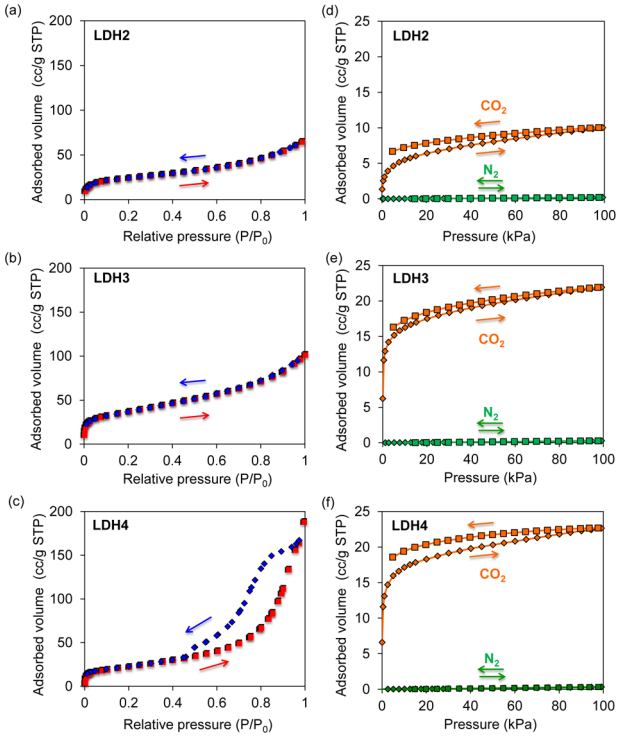

Figure 7. N_2 adsorption−desorption isotherms of (a) **LDH2**, (b) **LDH3**, and (c) **LDH4** measured at 77.35 K. CO_2 and N_2 adsorption−desorption isotherms of (d) **LDH2**, (e) **LDH3**, and (f) **LDH4** measured at 25 °C.

obtained for **LDH2−4** are about 5−10 times larger than that of commercially available LDH (12.3 m^2/g, Mg/Al = 3)[32] due to the small size of the LDH particles (Figure 3). In addition, these specific surface areas are close to the external surface area of LDH particles calculated based on the size and density of LDH (2.0 g/cm^3)[32] so that N_2 molecules are assumed not to enter the interlayer nanospace. The shapes of the N_2 adsorption−desorption isotherms of **LDH2** and **LDH3** can be categorized as being type II, indicating that they are neither microporous nor mesoporous. In contrast, the shape of N_2 adsorption−desorption isotherm of **LDH4** can be categorized as being type IV with a hysteresis loop; a type which has been often observed in mesoporous materials. As shown in its SEM image (Figure 3c), **LDH4** is composed of aggregates of thin LDH plates, which could lead to the formation of interparticle spaces.

As shown in adsorption−desorption isotherms for CO_2 and N_2 at 25 °C (Figure 7d−f), LDHs selectively incorporate CO_2 to the interlayer nanospace with capacities of **LDH2** < **LDH3** ≈ **LDH4**. Since Mg rich LDH is reported to promote base-catalyzed reactions,[42] the adsorption site of CO_2 must be basic Mg—OH. Therefore, **LDH4** shows the large capacity for CO_2 adsorption. In addition, as we discussed previously, the interlayer nanospace of **LDH4** is not densely occupied with water molecules and carbonate anions, so that it has the capacity to incorporate a larger quantity of CO_2 within interlayer nanospace.

Solid-State NMR Spectroscopy. To investigate further, solid-state NMR spectroscopies were performed for ^{13}C, ^{27}Al, and ^{17}O nuclei. As shown in Figure 8a, the ^{13}C CP/MAS NMR

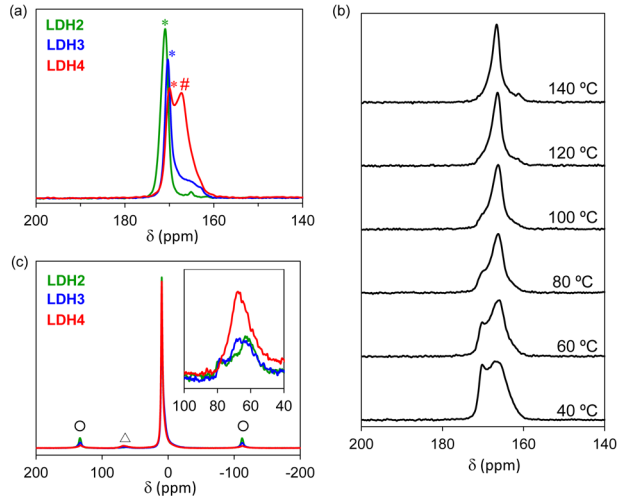

Figure 8. (a) ^{13}C CP/MAS NMR spectra of **^{13}C-LDH2**, **^{13}C-LDH3**, and **^{13}C-LDH4**. MAS speed was 10 kHz. Contact time and pulse delay were 5 ms and 15 s, respectively. (b) Variable temperature ^{13}C CP/MAS NMR spectra of **^{13}C-LDH4**. (c) ^{27}Al MAS NMR spectra of **^{13}C-LDH2**, **^{13}C-LDH3**, and **^{13}C-LDH4**. MAS speed was 16 kHz. Pulse delay was 2 s. Open circles at −110 and 130 ppm denote spinning side bands. Open triangle at 70 ppm donate impurity from tetrahedral aluminum.

spectrum of **^{13}C-LDH4** contains two distinct signals at 167 (indicated by hash mark) and 170 ppm (indicated by asterisk), whereas **^{13}C-LDH2** and **^{13}C-LDH3** contain a single intense peak at around 170−171 ppm (indicated by asterisks) although there is a low intensity peak around 165 ppm. Variable temperature NMR (Figure 8b) indicates that NMR signals of **^{13}C-LDH4** at 167 and 170 ppm merge to a single peak upon heating above 120 °C, so that the two NMR signals are derived from chemically exchangeable species. NMR signals at 167 and 170 ppm would be ascribed to HCO_3^-/CO_3^{2-} couple[43] or CO_3^{2-} interacting with brucite-like oxide layers in a different manner. As shown by XRD measurement (Figure 4), the basal spacing of **^{13}C-LDH4** is larger than those of **^{13}C-LDH2** and **^{13}C-LDH3**, so that interlayer carbonate anions are more mobile and various modes of motion should be available. In fact, T_1 relaxation times of carbonate anions of **^{13}C-LDH4** (19.2 s for 166.8 ppm and 26.4 s for 170.1 ppm) are much shorter than those of **^{13}C-LDH3** (110.0 s for 165.1 ppm and 116.9 s for 170.6 ppm) and **^{13}C-LDH2** (319.7 s for 171.1 ppm), revealing the high mobility of carbonate anion in **^{13}C-LDH4**.[44] ^{27}Al MAS NMR spectra of **^{13}C-LDH2**, **^{13}C-LDH3**, and **^{13}C-LDH4** are almost identical containing a single intense peak at around 10 ppm, which is typical of Al^{3+} with octahedral coordination. As seen in Figure 8c, ^{27}Al MAS NMR spectra are accompanied by a negligible signal at around 70 ppm (donated by open triangle), which is due to an impurity of Al^{3+} with square pyramid coordination. ^{27}Al NMR spectra suggest that Al^{3+} ions are well dispersed within the layered frameworks of LDHs, following the rule of Al—O—Al avoidance,[45] so that all Al^{3+}

dx.doi.org/10.1021/am5060405 | ACS Appl. Mater. Interfaces 2014, 6, 18352−18359

ions in LDH are connected to six Mg^{2+} ions through oxygen atoms. Al^{3+} ions contained in the layered frameworks of LDHs are considered to be the sites at which the carbonate anions exist as counterions, and ^{27}Al NMR studies revealed that the chemical environments of Al^{3+} ions are similar for **^{13}C-LDH2**, **^{13}C-LDH3**, and **^{13}C-LDH4**.

Moreover, ^{17}O MAS NMR studies proved the existence of the equilibrium involving carbonate anions and water. Figure 9

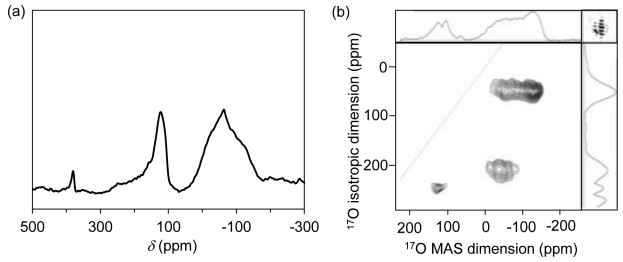

Figure 9. (a) ^{17}O MAS NMR spectra of carbonate-type LDH doped with ^{17}O-labeled water. MAS speed was 15 kHz. (b) ^{17}O 3QMAS NMR spectra of carbonate-type LDH doped with ^{17}O-labeled water. MAS speed was 15 kHz. Note that NMR signal at around 380 ppm derives from ZrO_2 rotor.

shows the ^{17}O MAS NMR spectrum of carbonate-type LDH.[46] The sample was prepared by immersing carbonate-type LDH in ^{17}O-labeled water for a week, followed by the removal of excess water in vacuum. It was anticipated that NMR inactive ^{16}O-oxygen-containing interlayer water of carbonate-type LDH could be exchanged with NMR active ^{17}O-labeled water, whereas ^{16}O-oxygen contained in the layered hydroxide framework was hardly exchanged with ^{17}O-oxygen contained in the ^{17}O-labeled water. Water molecule with free molecular motion usually provides a sharp ^{17}O MAS NMR signal at around 0 ppm.[47−49] In contrast, ^{17}O MAS NMR spectra of carbonate-type LDH does not show an NMR signal at 0 ppm, but contains two resolved signals at around −80 ppm and 100−200 ppm (Figure 9a). The NMR signal at around −80 ppm is typical of water molecules with reduced dynamics and symmetry of molecular motion,[47,48] and could be caused by the formation of a hydrogen bonded network between the interlayer water molecules and carbonate anions.[32] 3Q MAS NMR spectra[50] of carbonate-type LDH shows that the broad ^{17}O NMR signal at around −80 ppm involves at least two signals, presumably due to the different chemical environment of water (Figure 9b). More importantly, the other ^{17}O NMR signal at around 100−200 ppm can be ascribed to carbonate anions.[49] The carbonate anions originally contained in carbonate-type LDH is NMR inactive because the majority of its oxygen atoms are ^{16}O. However, there must exist an equilibrium involving interlayer carbonate anions and ^{17}O-labeled interlayer water, leading to the transfer of ^{17}O atom from water to carbonate anions. This result indicates that water molecules play an important role in the exchange reaction between interlayer carbonate anion and atmospheric CO_2. On the basis of these facts, the following reaction equations are formulated: eqs 1 and 2 indicate that atmospheric CO_2 adsorbed at the interlayer of LDH reacts with interlayer water, leading to the formation of protons and carbonate anions. The resulting carbonate anions replaces the carbonate anions already present in LDH (eq 3). Protons then react with carbonate anions leading to emission of CO_2 to the air. This mechanism is consistent with the previously proposed mechanism of decarbonation reaction of carbonate-type LDHs.[2]

$$CO_2(\text{air}) \rightleftharpoons CO_2(\text{interlayer}) \quad (1)$$

$$CO_2(\text{interlayer}) + H_2O(\text{interlayer}) \rightleftharpoons 2H^+(\text{interlayer}) + CO_3^{2-}(\text{interlayer}) \quad (2)$$

$$CO_3^{2-}(\text{interlayer}) + {}^{13}CO_3^{2-}(\text{anion of LDH}) \rightleftharpoons CO_3^{2-}(\text{anion of LDH}) + {}^{13}CO_3^{2-}(\text{interlayer}) \quad (3)$$

CONCLUSIONS

We have investigated the influence of the Mg/Al ratio of LDHs on the exchange between interlayer carbonate anion and atmospheric CO_2. It was found that magnesium rich LDH ($Mg_{0.8}Al_{0.2}(OH)_2(CO_3)_{0.1}\cdot yH_2O$) demonstrated extremely rapid exchange of carbonate anion, with the majority of the initially intercalated carbonate anion being replaced with atmospheric-CO_2-derived carbonate anions within 30 min. The use of various physicochemical techniques revealed that the decrease of charge density in the layered framework (i.e., increase of Mg/Al ratio) promotes the exchange reaction because of (i) increased vacancies in its interlayer space, (ii) increased CO_2 adsorption capacity from air, and (iii) increased mobility of carbonate anions within the interlayer. These results indicate that the unique interactions between CO_2 and LDH can be tuned simply by varying the chemical composition of LDH, implying that LDH is a promising material for CO_2 storage and/or separation.

EXPERIMENTAL SECTION

Materials. $Mg(NO_3)_2\cdot 6H_2O$ (min 99% purity, Kanto Chemical, Co., Ltd.), $Al(NO_3)_2\cdot 9H_2O$ (min 98% purity, Kanto Chemical, Co., Ltd.), Na_2CO_3 (min 99.8% purity, Nacalai Tesque, Inc.), NaOH (min 97% purity, Nacalai Tesque, Inc.), and 0.1 M HCl in propanol (Wako Pure Chemical Industries, Ltd.) were utilized as received. ^{13}C-labeled (^{13}C, 99%) Na_2CO_3 (Cambridge Isotope Laboratories, Inc.) and ^{17}O labeled (17O, 90%) water (RWE NUKEM, Ltd.) were utilized as received. Water was deionized using a Milli-Q Lab (Millipore), distilled using an Autostill WG220 (Yamato), and then degassed by boiling for 30 min. Degassed water was stored in a sealed glass bottle, and used for synthesis. Dry N_2 containing 395 ppm of CO_2 was purchased from Suzuki Shokan Co., Ltd.

Methods. SEM images were obtained using a Hitachi SU-8000 scanning electron microscope operating at an accelerating voltage of 5 kV. Powder XRD analysis was performed at a scan rate of 2θ = 2 degree/min using a Rigaku RINT 1200 diffractometer with Ni-filtered CuK_α radiation (λ = 1.5418 Å). XRD measurements were conducted at 25 °C under N_2 flow (0.1 L/min). The basal spacing corresponds to the d_{003} of the unit cell, which is the c-value of the subcell containing one interlayer space and one-third the LDH unit cell. The Mg/Al ratios contained in LDHs were determined by using inductively coupled plasma atomic emission spectroscopy (ICP-AES: Optima-2000, PerkinElmer) after fully dissolving LDH powder in 0.1 mol/L of nitric acid. TG analysis was performed using a RIGAKU Thermoplus TG8120 (RIGAKU Co., Ltd.) at 10 °C/min under dry N_2 flow (100 mL/min) over the range from room temperature to 600 °C using Al_2O_3 powder as a standard. In order to remove loosely bound water, each sample was placed inside the TG instrument and annealed at 40 °C under dry N_2 flow for 6 h. Relative humidity (RH) % was measured using a digital humidity/temperature meter (CUSTOM CTH-1100). FT-IR spectra were recorded using an FT-IR spectrometer (Spectrum One, PerkinElmer) at room temperature using an ATR accessory

(PerkinElmer L1200361, single reflection-type with Diamond/ZnSe top-plate). For relative humidity variation, N_2 gas was bubbled through water. Specific surface area was investigated by recording N_2 adsorption−desorption isotherms on an automatic adsorption instrument (Quantachrome Instrument, Autosorb-1 U.S.A.). For each measurement about 50−80 mg of sample was taken and degassed for 12 h at room temperature prior to the measurement. The adsorption−desorption isotherms were recorded at liquid nitrogen temperature 77.35 K. Specific surface areas were estimated by using the BET method. Adsorption (CO_2 and N_2) measurements at 25 °C were performed using BELSORP (BEL JAPAN, Inc.). For each measurement, about 200 mg of sample was taken and degassed for 12 h at room temperature prior to the measurement. High-resolution solid-state NMR experiments were carried out at 500.2, 125.7, 130.3, and 67.8 MHz for ^{1}H, ^{13}C, ^{27}Al, and ^{17}O respectively, using a JEOL ECA500 spectrometer. The instrument was equipped with a high power amplifier for proton decoupling and a cross-polarization/magic angle spinning (CP/MAS) probe. Samples were packed as powders in a ZrO_2 rotor (⌀ = 4 mm). Sample temperature was 300 ± 3 K unless otherwise noted. ^{13}C NMR spectra were externally referenced to the methyl carbon signal of hexamethylbenzene (17.4 ppm relative to TMS). ^{27}Al-NMR spectra were externally referenced to the aluminum signal of $AlCl_3$ in H_2O at 0 ppm. ^{17}O NMR spectra were externally referenced to the H_2O at 0 ppm. Torchia's pulse sequence was used for T_1 relaxation time measurements. For ^{17}O NMR experiments, 100 mg of carbonate-type LDH[46] were dispersed in 250 μL ^{17}O-labeled water. The suspension was stirred for 1 week to promote the exchange of interlayer water. The sample was dried in vacuum overnight, and supplied for ^{17}O NMR experiments. For 3QMAS ^{17}O NMR measurements, the spectral range was 80 kHz, and the duration time of T_1 was set at 66.7 μs for rotor-synchronizing. Pulse delay was 100 ms. NMR signals were accumulated 48000 times.

Monitoring IR Spectra of ^{13}C-LDHs. **^{13}C-LDHs** were placed inside a desiccator equipped with two channels for gas flow. Either dry N_2 gas containing 395 ppm of CO_2 (RH = 1.8% by humidity monitor) or wet N_2 gas containing 395 ppm of CO_2 (RH = 98% by humidity monitor) was utilized at a flow rate of 100 mL/min. For dry conditions, IR spectra of **^{13}C-LDHs** were measured in ATR mode immediately after being removed from the desiccator (within 2 min). For wet condition, IR spectra of **^{13}C-LDHs** were measured in ATR mode after drying the samples in vacuum at room temperature for 6 h.

Syntheses of LDHs by Coprecipitation.[36] Coprecipitation method was used to prepare three LDHs with Mg^{2+} and Al^{3+} ratio of 2, 3, and 4. A typical procedure is as follows. 0.3 M Na_2CO_3 was added dropwise to a stirred aqueous solution of $Mg(NO_3)_2{\cdot}6H_2O$ and $Al(NO_3)_2{\cdot}9H_2O$ in deionized water at 76 °C. Two M NaOH aq. was used to maintain the pH at 12. The reaction was aged for 17 h then the white solid was collected by filtration, and washed well with water and methanol. The product was dried in vacuum overnight, then stored in an atmosphere of dry N_2.

LDH2: 0.3 M aq. Na_2CO_3 (150 mL) was added to $Mg(NO_3)_2{\cdot}6H_2O$ (2.564 g) and $Al(NO_3)_2{\cdot}9H_2O$ (1.876 g) in deionized water (150 mL). Yield: 1.26 g;

LDH3: 0.3 M aq. Na_2CO_3 (180 mL) was added to $Mg(NO_3)_2{\cdot}6H_2O$ (3.077 g) and of $Al(NO_3)_2.9H_2O$ (1.501 g) in deionized water (150 mL). Yield: 1.20 g;

LDH4: 0.3 M aq. Na_2CO_3 (180 mL) was added to $Mg(NO_3)_2{\cdot}6H_2O$ (3.077 g) and of $Al(NO_3)_2.9H_2O$ (1.125 g) in deionized water (150 mL). Yield: 0.97 g.

Syntheses of Cl-LDHs by Anion Exchange.[32,37] LDH (800 mg) was added to EtOH (345 mL) and sonicated strongly to prepare a suspended solution. Dry N_2 was passed through the suspension (0.5 L/min) for 15 min, and then 0.1 M HCl in propanol (50.6 mL) was slowly added to the suspension. The mixture was stirred for 4 h under N_2 flow. The white solid was then collected by centrifugation (4000 rpm), and washed thoroughly with methanol. The product was dried in vacuum overnight, and stored in an atmosphere of dry N_2.

Cl-LDH2: Yield: 745 mg;

Cl-LDH3: Yield: 762 mg;

Cl-LDH4: Yield: 800 mg.

Syntheses of ^{13}C-LDHs by Anion Exchange.[32] Cl-LDH (517 mg) was dispersed in degassed water (32 mL) and N_2 was maintained bubbling through the suspension (0.5 L/min). After 15 min, $Na_2{}^{13}CO_3$ (1635 mg) dissolved in degassed water (96 mL) was added to the suspension and stirring was continued for 5 h with N_2 bubbling. The white solid was collected by centrifugation (4000 rpm), and washed thoroughly with degassed water. The product was dried in vacuum overnight, and stored in an atmosphere of dry N_2. The yields of **^{13}C-LDH2**, **^{13}C-LDH3**, and **^{13}C-LDH4** were essentially quantitative but were not accurately determined to avoid exposure of samples to air.

AUTHOR INFORMATION

Corresponding Authors

*E-mail: ISHIHARA.Shinsuke@nims.go.jp.

*E-mail: IYI.Nobuo@nims.go.jp.

Author Contributions

P.S. synthesized LDHs, measured IR and SEM, and analyzed carbonate anion exchange. S.I. measured XRD and TG. K.Y., K.D., S.O., M.T., and T.S. performed solid-state NMR studies. N.E. and R.S. performed elemental analyses. J.L., D.I., J.P.H., and K.A. discussed the results and assisted in the design of some of the experiments. B.P.B. and Y.Y. measured specific surface area. S.I. and N.I. directed the research. S.I. wrote the manuscript with input from all authors. All authors read the manuscript and have given approval to it.

Notes

The authors declare no competing financial interest.

ACKNOWLEDGMENTS

This research was partly supported by World Premier International Research Center Initiative on Materials Nanoarchitectonics and Grant-in-Aid for Scientific Research (B) (No. 22350090) from the Ministry of Education, Culture, Sports, Science and Technology (MEXT), Japan. Dr. Warashina (BEL JAPAN, Inc.) is acknowledged for adsorption measurement. Prof. Takahiro Iijima (Yamagata University) is acknowledged for fruitful discussions on 3QMAS NMR.

REFERENCES

(1) Duan, X.; Evans, D. G. *Layered Double Hydroxide*; Springer: Heidelberg, 2006.

(2) Iyi, N.; Matsumoto, T.; Kaneko, Y.; Kitamura, K. Deintercalation of Carbonate Ions from a Hydrotalcite-Like Compound: Enhanced Decarbonation Using Acid−Salt Mixed Solution. *Chem. Mater.* **2004**, *16*, 2926−2932.

(3) For example, hydrotalcite (Mg/Al), desautelsite (Mg/Mn), pyroaurite (Mg/Fe), stichtite (Mg/Cr), takovite (Ni/Al), and zaccagnaite (Zn/Al).

(4) Ma, R.; Liu, Z.; Takada, K.; Iyi, N.; Bando, Y.; Sasaki, T. Synthesis and Exfoliation of Co^{2+}—Fe^{3+} Layered Double Hydroxides: An Innovative Topochemical Approach. *J. Am. Chem. Soc.* **2007**, *129*, 5257−5263.

(5) Iyi, N.; Matsumoto, T.; Kaneko, Y.; Kitamura, K. A Novel Synthetic Route to Layered Double Hydroxides Using Hexamethylenetetramine. *Chem. Lett.* **2004**, *33*, 1122−1123.

(6) Bravo-Suárez, J. J.; Páez-Mozo, E. A.; Oyama, S. T. Review of the Synthesis of Layered Double Hydroxides: A Thermodynamic Approach. *Quim. Nova.* **2004**, *27*, 601−614.

(7) Iyi, N.; Sasaki, T. Deintercalation of Carbonate Ions and Anion Exchange of an Al-rich MgAl-LDH (Layered Double Hydroxide). *Appl. Clay Sci.* **2008**, *42*, 246−251.

(8) Iyi, N.; Yamada, H. One-step Conversion of CO_3^{2-}LDH (Layered Double Hydroxide) into Anion-exchangeable LDHs Using an Acetate-buffer/Salt Method. *Chem. Lett.* **2010**, *39*, 591−593.

(9) Bish, D. L. Anion-exchange in Takovite—Applications to other Hydroxide Minerals. *Bull. Mineral.* **1980**, *103*, 170−175.
(10) Sasai, R.; Norimatsu, W.; Matsumoto, Y. Nitrate-ion-selective Exchange Ability of Layered Double Hydroxide Consisting of Mg^{II} and Fe^{III}. *J. Hazard Mater.* **2012**, *215*−*216*, 311−314.
(11) Miyata, S.; Hirose, T. Adsorption of N_2, O_2, CO_2, and H_2 on Hydrotalcite-Like System: Mg^{2+}—Al^{3+}—$(Fe(CN)_6)^{4-}$. *Clays Clay Miner.* **1978**, *26*, 441−447.
(12) Pavan, P. C.; Gomes, G. D.; Valim, J. B. Adsorption of Sodium Dodecyl Sulfate on Layered Double Hydroxides. *Microporous Mesoporous Mater.* **1998**, *21*, 659−665.
(13) Hutson, N. D.; Speakman, S. A.; Payzant, E. A. Structural Effects on the High Temperature Adsorption of CO_2 on a Synthetic Hydrotalcite. *Chem. Mater.* **2004**, *16*, 4135−4143.
(14) Ram Reddy, M. K.; Xu, Z. P.; Lu, G. Q.; Diniz da Costa, J. C. Layered Double Hydroxides for CO_2 Capture: Structure Evolution and Regeneration. *Ind. Eng. Chem. Res.* **2006**, *45*, 7504−7509.
(15) Wang, Q.; Gao, Y.; Luo, J.; Zhong, Z.; Borgna, A.; Guo, Z.; O'Hare, D. Synthesis of Nano-sized Spherical Mg_3Al—CO_3 Layered Double Hydroxide as a High-Temperature CO_2 Adsorbent. *RSC Adv.* **2013**, *3*, 3414−3420.
(16) Gao, Y.; Zhang, Z.; Wu, J.; Yi, X.; Zheng, A.; Umar, A.; O'Hare, D.; Wang, Q. Comprehensive Investigation of CO_2 Adsorption on Mg—Al—CO_3 LDH-derived Mixed Metal Oxides. *J. Mater. Chem. A* **2013**, *1*, 12782−12790.
(17) Cavani, F.; Trifirò, F. F.; Vaccari, A. Hydrotalcite-type Anionic Clays: Preparation, Properties and Applications. *Catal. Today* **1991**, *11*, 173−301.
(18) Sels, B.; De Vos, D.; Buntinx, M.; Pierard, F.; Kirsch-De Mesmaeker, A.; Jacobs, P. Layered Double Hydroxides Exchanged with Tungstate as Biomimetic Catalysts for Mild Oxidative Bromination. *Nature* **1999**, *400*, 855−857.
(19) He, S.; An, Z.; Wei, M.; Evans, D. G.; Duan, X. Layered Double Hydroxide-based Catalysts: Nanostructure Design and Catalytic Prformance. *Chem. Commun.* **2013**, *49*, 5912−5920.
(20) Li, F.; Tan, Q.; Evans, D. G.; Duan, X. Synthesis of Carbon Nanotubes using a Novel Catalyst Derived from Hydrotalcite-like Co-Al Layered Double Hydroxide Precursor. *Catal. Lett.* **2005**, *99*, 151−156.
(21) Sels, B. F.; De Vos, D. E.; Jacobs, P. A. Hydrotalcite-like Anionic Clays in Catalytic Organic Reactions. *Catal. Rev.* **2001**, *43*, 443−488.
(22) Teramura, K.; Iguchi, S.; Mizuno, Y.; Shishido, T.; Tanaka, T. Photocatalytic Conversion of CO_2 in Water over Layered Double Hydroxides. *Angew. Chem., Int. Ed.* **2012**, *51*, 8008−8011.
(23) Du, X.; Zhang, D.; Gao, R.; Huang, L.; Shi, L.; Zhang, J. Design of Modular Catalysts Derived from NiMgAl-LDH@*m*-SiO_2 with Dual Confinement Effects for Dry Reforming of Methane. *Chem. Commun.* **2013**, *49*, 6770−6772.
(24) Ishihara, S.; Iyi, N.; Tsujimoto, Y.; Tominaka, S.; Matsushita, Y.; Krishnan, V.; Akada, M.; Labuta, J.; Deguchi, K.; Ohki, S.; Tansho, M.; Shimizu, T.; Ji, Q.; Yamauchi, Y.; Hill, J. P.; Abe, H.; Ariga, K. Hydrogen-Bond-Driven 'Homogeneous Intercalation' for Rapid, Reversible, and Ultra-Precise Actuation of Layered Clay Nanosheets. *Chem. Commun.* **2013**, *49*, 3631−3633.
(25) Ogawa, M.; Kuroda, K. Photofunctions of Intercalation Compounds. *Chem. Rev.* **1995**, *95*, 399−438.
(26) Peak, S.-M.; Oh, J.-M.; Choy, J.-H. A Lattice-Engineering Route to Heterostructured Functional Nanohybrids. *Chem.—Asian J.* **2011**, *6*, 324−338.
(27) Káfuňková, E.; Lang, K.; Kubát, P.; Klementová, M.; Mosinger, J.; Šlouf, M.; Troutier-Thuilliez, A.-L.; Leroux, F.; Verneyf, V.; Taviot-Guého, C. Porphyrin-Layered Double Hydroxide/Polymer Composites as Novel Ecological Photoactive Surfaces. *J. Mater. Chem.* **2010**, *20*, 9423−9432.
(28) Ishihara, S.; Iyi, N.; Labuta, J.; Deguchi, K.; Ohki, S.; Tansho, M.; Shimizu, T.; Yamauchi, Y.; Sahoo, P.; Naito, M.; Abe, H.; Hill, J. P.; Ariga, K. Naked-Eye Discrimination of Methanol from Ethanol Using Composite Film of Oxoporphyrinogen and Layered Double Hydroxide. *ACS Appl. Mater. Interfaces* **2013**, *5*, 5927−5930.
(29) Liu, Y.; Wang, N.; Caro, J. In Situ Formation of LDH Membranes of Different Microstructures with Molecular Sieve Gas Selectivity. *J. Mater. Chem. A* **2014**, *2*, 5716−5723.
(30) Alcantara, A. C. S.; Aranda, P.; Darder, M.; Ruiz-Hitzky, E. Bionanocomposites Based on Alginate−Zein/Layered Double Hydroxide Materials as Drug Delivery Systems. *J. Mater. Chem.* **2010**, *20*, 9495−9504.
(31) Tanaka, M.; Aisawa, S.; Hirahara, H.; Narita, E.; Yin, S.; Sato, T. Cellular Uptake Behavior of Fluorescein: Intercalated Layered Double Hydroxide. *Funct. Mater. Lett.* **2012**, *5*, 1260003.
(32) Ishihara, S.; Sahoo, P.; Deguchi, K.; Ohki, S.; Tansho, M.; Shimizu, T.; Labuta, J.; Hill, J. P.; Ariga, K.; Watanabe, K.; Yamauchi, Y.; Suehara, S.; Iyi, N. Dynamic Breathing of CO_2 by Hydrotalcite. *J. Am. Chem. Soc.* **2013**, *135*, 18040−18043.
(33) Falkowski, P.; Scholes, R. J.; Boyle, E.; Canadell, J.; Canfield, D.; Elser, J.; Gruber, N.; Hibbard, K.; Högberg, P.; Linder, S.; Mackenzie, F. T.; Moore, B.; Pedersen, T.; Rosenthal, Y.; Seitzinger, S.; Smetacek, V.; Steffen, W. The Global Carbon Cycle: A Test of Our Knowledge of Earth as a System. *Science* **2000**, *290*, 291−296.
(34) Berner, R. A.; Lasaga, A. C.; Garrels, R. M. The Carbonate-Silicate Geochemical Cycle and Its Effect on Atmospheric Carbon-dioxide over the Past 100 Million Years. *Am. J. Sci.* **1983**, *283*, 641−683.
(35) The Slow Carbon Cycle. http://earthobservatory.nasa.gov/Features/CarbonCycle/page2.php (NASA, accessed 4 July 2014).
(36) Tadanaga, K.; Furukawa, Y.; Hayashi, A.; Tatsumisago, M. Effect of Mg/Al Ratio on Hydroxide Ion Conductivity for Mg-Al Layered Double Hydroxide and Application to Direct Ethanol Fuel Cells. *J. Electrochem. Soc.* **2012**, *159*, B368−B370.
(37) Iyi, N.; Yamada, H.; Sasaki, T. Deintercalation of Carbonate Ions from Carbonate-type Layered Double Hydroxides (LDHs) using Acid−Alcohol Mixed Solutions. *Appl. Clay Sci.* **2011**, *54*, 132−137.
(38) Tossell, J. A. H_2CO_3 and Its Oligomers: Structures, Stabilities, Vibrational and NMR Spectra, and Acidities. *Inorg. Chem.* **2006**, *45*, 5961−5970.
(39) Miyata, S. Physico-Chemical Properties of Synthetic Hydrotalcites in Relation to Composition. *Clays Clay Miner.* **1980**, *28*, 50−56.
(40) Hibino, T.; Yamashita, Y.; Kosuge, K.; Tsunashima, A. Decarbonation Behavior of Mg—Al—CO_3 Hydrotalcite-like Compounds during Heat Treatment. *Clays Clay Miner.* **1995**, *43*, 427−432.
(41) Stanimirova, T.; Piperov, N.; Petrova, N.; Kirov, G. Thermal Evolution of Mg—Al—CO_3 Hydrotalcites. *Clay Miner.* **2004**, *39*, 177−191.
(42) Constantino, V. R. L.; Pinnavaia, T. J. Basic Properties of $Mg^{2+}_{1-x}Al^{3+}_x$ Layered Double Hydroxides Intercalated by Carbonate, Hydroxide, Chloride, and Sulfate Anions. *Inorg. Chem.* **1995**, *34*, 883−892.
(43) Gottlieb, H. E.; Kotlyar, V.; Nudelman, A. NMR Chemical Shifts of Common Laboratory Solvents as Trace Impurities. *J. Org. Chem.* **1997**, *62*, 7512−7515.
(44) Hayashi, S.; Suzuki, K.; Hayamizu, K. High-Resolution Solid-State ^{13}C Nuclear Magnetic Resonance Study of the Dynamic Behaviour of Tetramethylammonium Ions Trapped in Zeolites. *J. Chem. Soc., Faraday Trans. 1* **1989**, *85*, 2973−2982.
(45) Sideris, P. J.; Blanc, F.; Gan, Z.; Grey, C. P. Identification of Cation Clustering in Mg—Al Layered Double Hydroxides Using Multinuclear Solid State Nuclear Magnetic Resonance Spectroscopy. *Chem. Mater.* **2012**, *24*, 2449−2461.
(46) Note that carbonate-type LDH (Mg/Al = 2) used here were prepared by hydrothermal method. See: Sasai, R.; Matsuoka, Y.; Sato, H.; Moriyoshi, C.; Kuroiwa, Y. Abnormally Large Thermal Vibration of Chloride Anions Incorporated in Layered Double Hydroxide Consisting of Mg and Al (Mg/Al = 2). *Chem. Lett.* **2013**, *42*, 1285−1287.
(47) Boykin, D. W. *^{17}O NMR Spectroscopy in Organic Chemistry*; CRC Press: Boca Raton, FL, 1991.
(48) Yamada, K. *Proc. Soc. Solid-State NMR Mater.* **2013**, *54*, 27.

(49) http://www.science-and-fun.de/tools/17o-nmr.html (accessed 1 May 2014).
(50) Medek, A.; Harwood, J. S.; Frydman, L. Multiple-Quantum Magic-Angle Spinning NMR: A New Method for the Study of Quadrupolar Nuclei in Solid. *J. Am. Chem. Soc.* **1995**, *117*, 12779−12787.